

Measures to reduce the residual field and field gradient inside a magnetically shielded room by a factor of more than 10

Jens Voigt, Silvia Knappe-Grüneberg, Allard Schnabel, Rainer Körber, and Martin Burghoff

Physikalisch-Technische-Bundesanstalt (PTB), Abbestr. 2-12, 10587 Berlin, Germany (✉ jens.voigt@ptb.de, +49 30 3481 7716)

Abstract

Very low residual magnetic field and field gradients are essential for a number of high resolution fundamental physical experiments and for further improvement of very sensitive magnetic measurement devices. The scope ranges from spin precession experiments, e.g. with ^3He or neutrons, to biomagnetic measurements, like magnetoencephalograms, and to low field MR spectroscopy. One method of reducing environmental magnetic noise is to use a magnetically shielded room (MSR). Here, measures are demonstrated to improve residual field and field gradient inside a common MSR by a factor of more than 10 by a specific degaussing procedure, material selection of prefabricated parts and active shielding. The process is independent of the shielding factor and works also properly for heavily shielded rooms.

Keywords: magnetic shielding, magnetic shielded room, msr, residual field, residual field gradient, degaussing, demagnetization

© 2013 Polish Academy of Sciences. All rights reserved

1. Introduction

High-resolution magnetic measurements, where signals in the range of a few femtotesla have to be detected, need an environment with low magnetic disturbances. Examples of such high resolution experiments are spin experiments with ^3He or ^{129}Xe [1], neutrons [2,3], ultra-low field NMR [4], or MRI [5] or biomagnetic recordings [6]. Each of these experiments has special magnetic requirements, like low residual magnetic fields, low magnetic field gradients and/or low residual field drifts. For example, the lifetime of the spin precession depends directly on the gradients over the sample volume. Additionally, each experimental setup vibrates with an eigenfrequency, e.g. activated by impact noise. This movement in a gradient field causes a periodic field change which is proportional to the product of the magnetic field gradient and the displacement. Such an artifact can dominate the system noise below 30 Hz where biomagnetic signals like magnetocardiograms and magnetoencephalograms have their main signal power [7]. Hence, the reduction of the magnetic field gradient and the mechanical vibrations are essential for low noise recordings.

A common method to reduce external magnetic disturbances, due to urban magnetic field noise and the Earth's magnetic field, is the use of a magnetically shielded room (MSR) made of high permeability ferromagnetic walls, e.g. Mu-metal [8]. Typically, the performance of an MSR is characterized by the shielding factor. The shielding factor depends on the frequency, the permeability, the number of the damping layers and on their geometric shape [9].

However, the static residual field inside MSR is dominated by the remanent field of the shielding walls and cannot be deduced from the quasi-static shielding factor. For example, for a common two Mu-metal + 1 aluminum layer MSR, like the *Ak3b* from VAC/Germany, the quasi static shielding factor is about 100. The residual magnetic field in the center of such an MSR is about 50 nT after delivery. That is a factor of 10 lower than expected when attenuating the Earth's field by 100 times. Typically, the gradient in such an MSR is below 30 pT/mm.

In 2010, a special *Ak3b* MSR was installed at PTB Berlin in the "Zuse" building by VAC. This MSR called *Zuse-MSR* consists of two layers of Mu-metal and a combined RF-eddy current shield made of copper-plated aluminum. The walls enclose a walk-in space of 2.5 m x 2.5 m x 2.3 m. Several methods were applied during the setup of the *Zuse-MSR* in order to reduce the residual field and field gradient by a factor of more than 10 times compared to other MSR with 2+1 layers.

2. Methods

The first measure for improving the performance of the MSR has to start already during assembly of the MSR. The other measures for increasing the performance can be carried out after assembly and during the usage of the MSR. For an existing MSR, it is recommended to evaluate the influence of the different sources of magnetic disturbances and selecting the necessary sequences of improvement.

1st measure - Magnetic test of all used equipment during assembly of the MSR

The residual field and the field gradient in an MSR mainly depend on the remanent field of the Mu-metal walls and the installed equipment. The grey areas in figure 1 illustrate the measured values inside *Zuse-MSRs* in a volume of 1 m³. For comparison, the ranges for a 7+1 layer MSR at PTB Berlin (*BMSR-2*) [10] and an *Ak3b* build for PTB in 1999 (*AMSR*) are shown. In addition, for typical assembly parts the magnetic moments are shown. Based on these measured values, the distance on the depending contribution of those parts onto the magnetic field and gradient are calculated using a dipole model. The magnetic disturbance due to accessories should be negligible. Hence, the permissible magnetic moment of an item depends on its local position inside the MSR, refer to fig. 1.

In our experience, the magnetic moment of such accessories are spread widely. Particularly, items made of compound material, like brass or stainless steel, show a variation in the magnetic moment over 2 to 3 orders of magnitude. Therefore, all auxiliary equipment inside an MSR, like screws, bolts, wires or connectors, were tested by a SQUID system before assembly. It doesn't matter if these parts were necessary for the MSR, or whether they belong to a separate experiment setup.

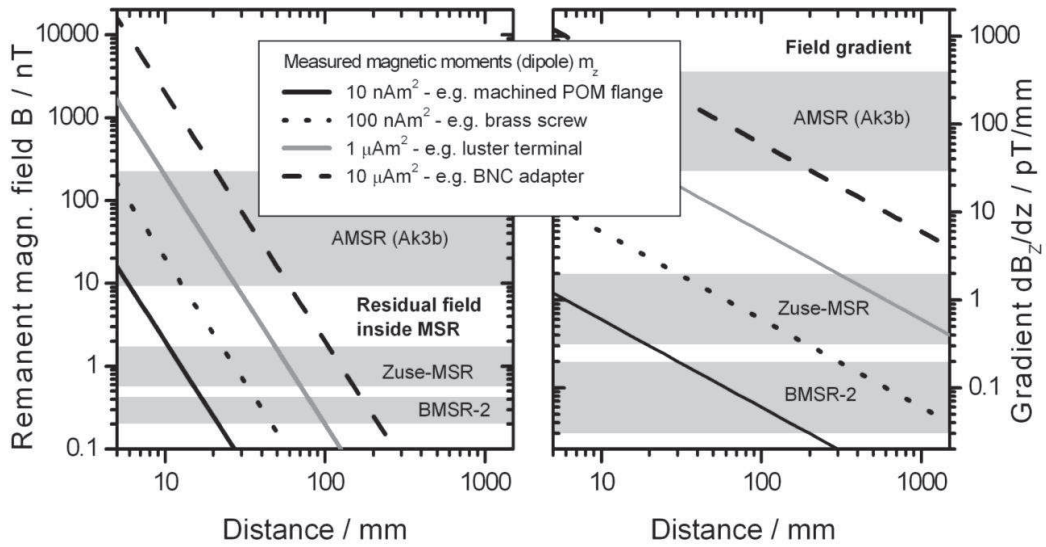


Fig. 1. Correlation between magnetic dipoles, used in several MSRs and the resultant residual magnetic field and field gradient. The gray areas represent the measured values inside three MSRs in a volume of 1 m³. The magnetic moment of typical assembly parts were measured. Their contribution to the remanent magnetic field (left) and magnetic field gradient (right) as a function of distance is calculated using a dipole model.

A first rough check of the magnetic quality can be done with a fluxgate. Using a simple dipole model, one can assume a rule of thumb: At a distance of 10 mm a perpendicular component B_z of 20 nT results from a magnetic moment of 100 nAm². Tests with higher resolution are difficult to perform, because commercial magnetic measurement systems, like a Gouy balance, require a very small, fixed sample size. Thus, we used a SQUID system which was developed to measure magnetic sources inside a human body [11]. Here, the sample size can be up to 1 m. The resolution limit is in the order of 5 nAm² and depends on the conductivity of the sample.

2nd measure – Setup of a degaussing procedure of the MSR

After the 1st improvement step, the residual field left inside the *Zuse-MSR* is determined by the magnetization of the Mu-metal wall. The magnetization can be reduced by degaussing. Therefore, a linearly decreasing sinusoidal current is applied to the *Zuse-MSR* degaussing coil system illustrated in figure 2a. The degaussing function has to meet two conditions for each local area of the shielding walls: a) the maximum current amplitude must be sufficient to achieve saturation, and b) the step size between two neighboring peak values has to be small enough to obtain a local 50:50 distribution of the domain orientation. The current amplitude, ranges from a peak value of 21 A * 5 windings down to a few milliampere using 2000 periods. In order to apply a high current to a large inductive load (about 1.5 mH per shell) a power amplifier (Rohrer/Germany) [6] is used. The output current is controlled by a free programmable function generator consisting of a PC with a 16-bit digital to analog converter [12, 13]. The degaussing setup is illustrated in figure 2b.

The degaussing frequency is 10 Hz as a compromise between the maximum current and the coil inductance, the skin depth and thickness of the Mu-metal layers and a convenient DC filter. Typical perturbation signals of the amplifier, like drift, offset and noise causes poor reproducibility of the demagnetization result, i.e. the residual magnetic field. Particularly, a tiny dc-offset would result in an imbalanced orientation of the domains and, therefore, in a higher residual field. Thus, a distortion-free transformer and multi-stage filtering are used. The skindepth is about 0.7 mm, assuming a degaussing frequency of 10 Hz, a resistivity of $55 \cdot 10^{-6} \Omega \text{ cm}$ [14] and a magnetic permeability of the used Mu-metal sheets of about 30000 [14]. This is sufficient to degauss the *Zuse-MSR* walls, each consisting of four sheets with a thickness of 0.75 mm.

One of the most important components is the degaussing coil setup. This setup should be able to saturate the whole Mu-metal walls. To avoid interaction during degaussing between saturated and nonsaturated parts, the magnetic field inside the Mu-metal should be uniform. For a block-shaped MSR this is not feasible. Hence, the PTB proposed degaussing coils encircling the twelve edges of each layer as shown in fig. 2a. The serial connection of four coils in one spatial direction behaves like a large toroidal coil with 4 Mu-metal walls as a core (gray in fig. 2b). Therefore the flux density inside the four walls has an almost identical magnetic path length which results in a homogeneous magnetization. The generated flux is mainly inside the Mu-metal walls with a negligible stray magnetic field entering the room and magnetizing the other two remaining walls. However, at least two separate degaussing sequences with two of the three coil sets of figure 2a are necessary to degauss all six walls of one layer.

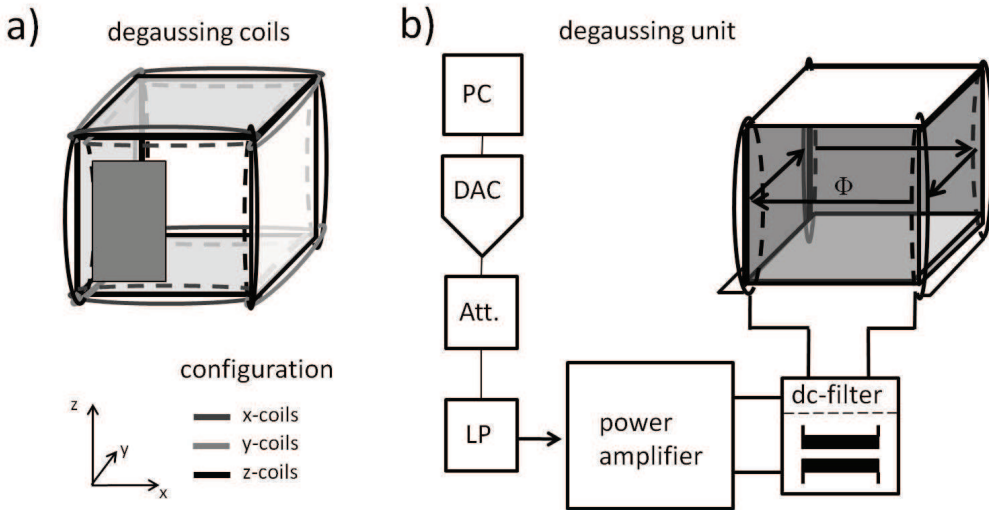


Fig. 2. Degaussing coil configurations of the *Zuse-MSR* (a) and degaussing unit (b).

3rd measure – Automating the degaussing procedure

Frequently, the Mu-metal walls are magnetized during maintenance work or experiments with additional magnetic fields. Therefore the degaussing was additionally automated by using a PXI system, LabVIEW software and six high current switches for the degaussing coils (x-, y- and z for the inside and outside layer) controlled by a microcontroller. This feature enables the possibility of a one button degaussing and of incorporating the degaussing procedure into measurement sequences, like low-field NMR. This is important to guarantee the reproducibility of the residual field before an actual experiment, independent of previous activities inside the MSR. Experiments using magnetic fields with different field strength and directions can be done automatically without any staff interaction.

4th measure - mechanical damping of the floor assembly of the MSR and installation of mechanical support connectors

In order to avoid large amplitudes of disturbances due to mechanical vibration (see fig. 3) a mechanical damping of the floor below the MSR is essential. One important step is the mechanical isolation of the floor assembly of the MSR from the surrounding floor to reduce vibrations of the MSR generated by personnel walking around the MSR.

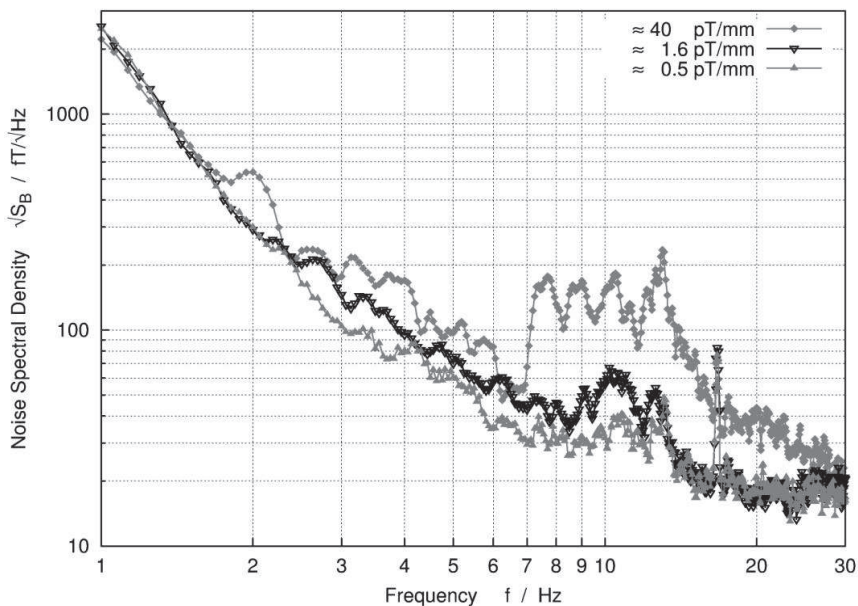


Fig. 3. The noise spectral density measured with a vertical sensitive SQUID magnetometer for three different field homogeneities in the center of the Zuse-MSR. Artifacts between 7 Hz and 30 Hz occur due to mechanical vibrations of the magnetic sensor in the gradient field. The peak at 16 $\frac{2}{3}$ Hz is generated by the German railway.

Even with mechanical damping of the floor assembly, some residual vibrations in the range of some micrometers appear. These vibrations lead to erroneous signals in the magnetic sensors, e.g. a displacement of 5 μm in a gradient field of 40 pT/mm will end up in a magnetic field change of 200 fT. This effect can be reduced, if the sensor and the source of the gradient field make the same movement. Therefore in the *Zuse-MSR*, a number of mechanical support connectors are installed in the wall frame in order to provide a stiff coupling between the Mu-metal walls, sensor and experimental setup.

5th measure – installation of active shielding

The measurement of the low frequency noise inside the new *Zuse-MSR* shows that a shielding factor of 100 at 0.01 Hz is insufficient to suppress the Berlin urban noise entirely (fig. 4). The main component of disturbances occurring in the z-axis is caused by the Berlin subway. It is reduced by an active shielding system. This consists of compensation coils with maximally $0.6 A_{\text{rms}} * 1$ ampere-turns, installed outside the MSR, and a fluxgate in a negative feedback circuit. The improvement by the active shielding is shown in fig. 4. Note that the active shielding should not interact with the degaussing procedure.

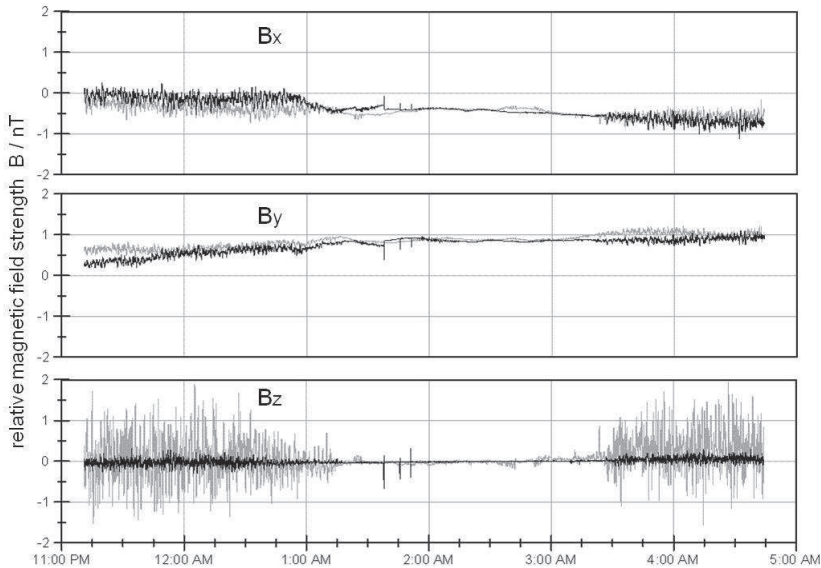


Fig. 4. Time courses of the relative magnetic field components B_x , B_y , B_z measured inside Zuse-MSR with a vector SQUID system. The gray time course shows the field drift without active shielding. The high noise floor in z-direction is mainly caused by the subway. The subway break at night can be seen clearly. Marked in black, the time courses of all three magnetic components are shown with active shielding for the z-axes. The active shielding during the daytime leads to a similar noise level to that at night when the subway takes a break. The spikes during the night are artifacts caused by the feedback circuit unable to compensate for fast changing magnetic field disturbances.

6th measure – installation of an air-conditioning system

Temperature changes in the Mu-metal walls lead to drifts of the residual magnetic field inside the MSR. Possible reasons are thermally induced equalizing currents or mechanical movement and stress of the Mu-metal walls. Inside the *BMSR-2*, the change of 1 Kelvin results in a magnetic field drift of around 5 pT. To avoid or to minimize these influences, an air-conditioning system was installed.

3. Results

The improvement of the residual field and field gradient due to measures 1 and 2 was characterized by a specific PTB vector SQUID system [15]. This SQUID system achieves an absolute magnetic field measurement with an uncertainty of < 50 pT at DC. It was moved in a 3D grid to determine the static magnetic field distribution, see figures 5 and 6. Due to the height of the SQUID system, the lower half of the *Zuse-MSR* was measured only. It was found that successive degaussing in x-, y-, z-direction of the complete shield improves the residual field significantly.

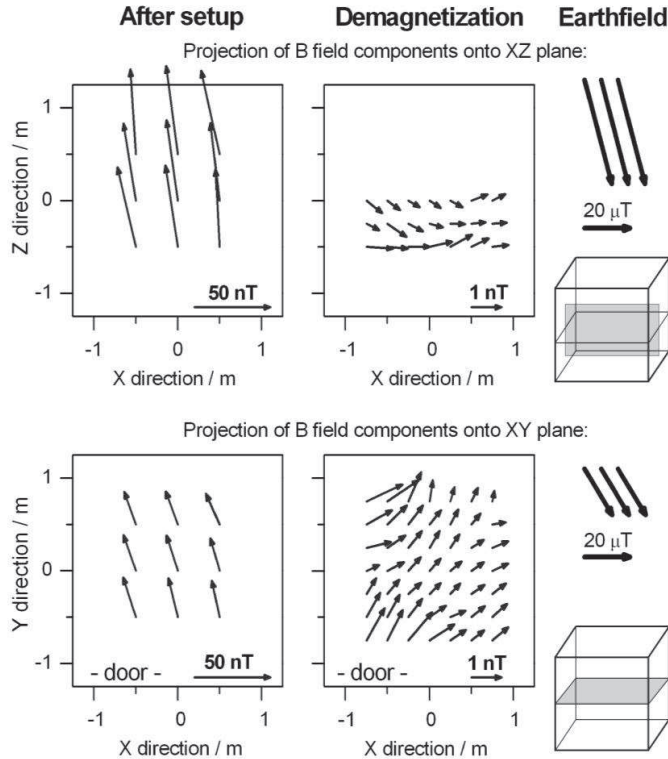


Fig. 5. Magnetic field map inside *Zuse-MSR*. Above: B_x and B_z components shown as projections onto the vertical plane. Below: projection of the B_x and B_y components onto a horizontal plane. Left: After installation of the MSR, using a fluxgate. Right: Result after degaussing using a SQUID system. Both measurements were performed at night during the subway break. Root points represent the measurement position. The origin corresponds to the center of the room.

After degaussing, the residual field is less than 1.5 nT with a gradient below 2 pT/mm in a volume of 1 m³. Compared with the static magnetic field inside a common 2+1 MSR with 50 nT residual field and < 30 pT/mm field gradient, this is an essential improvement by a factor of more than 15. Note that the field direction inside an MSR is usually not parallel to the Earth's magnetic field.

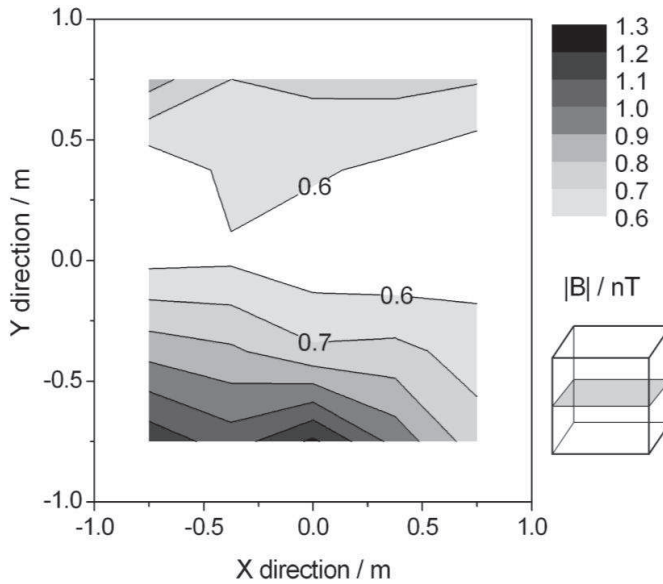


Fig. 6. Magnitude of the residual magnetic field $|B|$ inside the Zuse-MSR after degaussing, measured at night. Shown is the central X-Y plane of the chamber. The high amplitude at the front right side is caused by the pneumatic buttons for open, close and security ventilation of the door mechanism, which still contains magnetically contaminated components, like springs.

The achieved residual field is so low now that the subway disturbances dominate during the daytime. Therefore, the magnetic field distribution shown in figs. 5, right, and 6 are measured at night during the subway break.

In fig. 4, the time courses (gray) of the magnetic field components B_x , B_y , B_z measured inside Zuse-MSR with the vector SQUID system are shown during the daytime and nighttime. Marked in black, the time courses of all three magnetic components are shown with an active shielding for the z-axis, as proposed in measure 5. An improvement of about 7 times can be detected during the daytime for these field drifts.

Fig. 7 depicts the noise spectral density to demonstrate the efficiency of the shielding of Zuse-MSR. The magnetic noise inside the Zuse-MSR is compared with the noise inside the 7+1 layered shielding BMSR-2 at PTB without active shielding. It can be seen that for frequencies above 10 Hz, the Zuse-MSR is close to the performance of BMSR-2. For lower frequencies, the magnetic noise inside the BMSR-2 is much lower due to the higher quasi-static shielding factor.

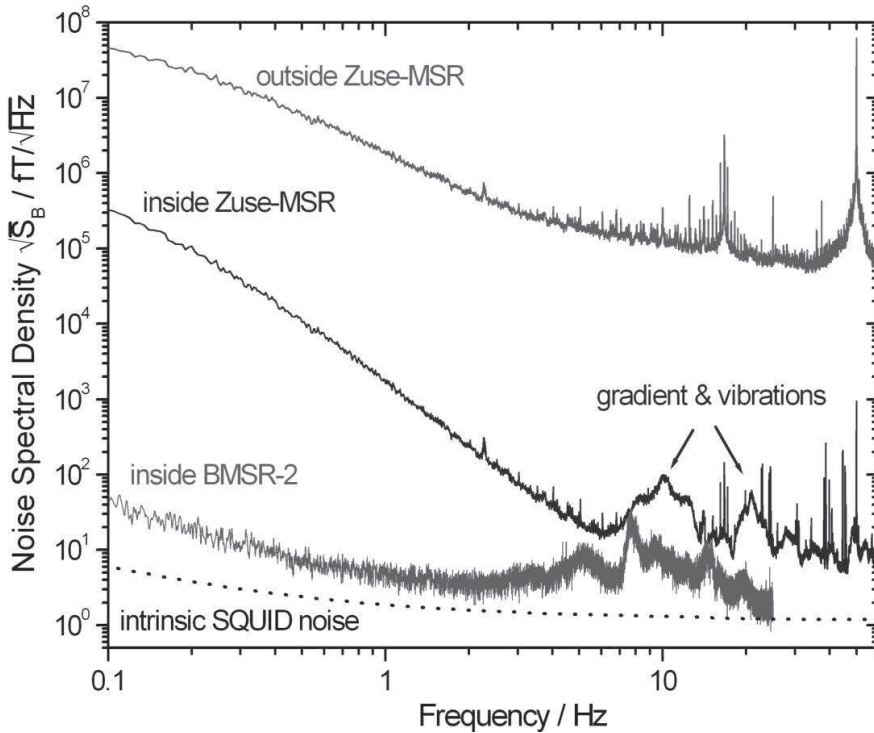


Fig. 7. Day time magnetic field noise inside BMSR-2 and Zuse-MSR measured with a SQUID system, compared to the surrounding urban field measured with a fluxgate. The behavior of the noise inside the Zuse-MSR is typical for a 2+1 layer MSR. The shielding factor at 0.1 Hz measured by the manufacturer is around 100 for the Zuse-MSR and 10^6 for BMSR-2.

4. Conclusion

The residual field and field gradients inside the new MSR made by VAC at PTB are reduced by at least one order of magnitude compared to a conventional MSR. This was accomplished by careful selection of the material used inside the inner Mu-shield and by a new integrated degaussing coil design proposed by PTB. The achieved residual field in a volume of 1 m^3 is less than 1.5 nT with a gradient below 2 pT/mm. This is a significant improvement compared to other existing *Ak3b* MSRs. In addition, the magnetic field drift in an MS can be reduced significantly by active shielding.

Parts of these results were successfully applied to an existing magnetic shield used for the search for an electric dipole moment of the neutron (nEDM) at the Paul Scherrer Institute, Switzerland. Here, a new degaussing system and equipment selection led to a significant improvement of the experiment [2].

Acknowledgement

This work is supported by the Federal Ministry of Education and Research, Bernstein Focus Neurotechnology, Project number 01GQ0852 and by the German Research Foundation (DFG), Project BU-1037/3-1.

References

- [1] Gemmel, C., et al. (2010). Limit on Lorentz and CPT violation of the bound neutron using a free precession. *Physical Review*, 11. 111901-1 - 111901-5
- [2] Baker, C. A., et al. (2011). The search for the neutron electric dipole moment at the Paul Scherrer Institute. *Physics Procedia*. 17. 159-167
- [3] Altarev, I., et al. (2012). A next generation measurement of the electric dipole moment of the neutron at the FRM II. *Il Nuovo Cimento 35 C 122*)
- [4] Höfner, N., et al. (2011). Are brain currents detectable by means of Low-Field NMR? - a phantom study - *Magnetic Resonance Imaging*. 29. 1365-1373
- [5] Hilschenz, I., et al. (2012). Magnetic resonance imaging at frequencies below 1 kHz. *Magnetic Resonance Imaging*. doi: 10.1016/j.mri.2012.06.014
- [6] Burghoff, M., et al. (2009). SQUID SYSTEM FOR MEG AND LOW FIELD MAGNETIC RESONANCE. *Metrology and Measurement systems*. 16. 3. 371-375
- [7] Hari, R., et al. (1997) Human cortical oscillations: a neuromagnetic view through the skull. *Trends Neurosci*. 20. 44-49
- [8] Cohen, D., et al. (1967). A Shielded Facility for Low Level Magnetic Measurements. *J. Appl. Phys.* 38. doi.org/10.1063/1.1709590,
- [9] Summer, T. J. (1987). Convectional magnetic shielding. *J. Phys. D: Appl. Phys.* 20.
- [10] Bork, J., et al. (2000). The 8-layered magnetically shielded room of the PTB. *Biomag Proceedings*. 970-973
- [11] Burghoff, M., et al. (2004). Discrimination of multiple sources using a squid vector magnetometer. *Biomag Proceedings*. 99-100
- [12] Thiel, F., et al. (2007). Demagnetization of magnetically shielded rooms, *Rev. Sci. Instrum.* 78. doi: 10.1063/1.2713433
- [13] Schnabel, A., et al. (2008). Crucial parameters for better degaussing of magnetically shielded rooms. Biomag poster,
- [14] <http://www.vacuumschmelze.de/index.php?id=497>, (January 2013)
- [15] Burghoff, M., et al. (1999). A Vector Magnetometer Module for Biomagnetic Application. *IEEE Appl. Superconductivity*. 9. 4069-4072.